Mineralogical Magazine, December 2011, Vol. 75(6), pp. 2813–2822

Fluorine-, yttrium- and lanthanide-rich cerianite-(Ce) from carbonatitic rocks of the Kerimasi volcano and surrounding explosion craters, Gregory Rift, northern Tanzania

A. N. Zaitsev[1,2,*], A. R. Chakhmouradian[3], O. I. Siidra[4], J. Spratt[2], C. T. Williams[2], C. J. Stanley[2], S. V. Petrov[5], S. N. Britvin[4] and E. A. Polyakova[1]

[1] Department of Mineralogy, Faculty of Geology, St Petersburg State University, University Emb., 7/9, St Petersburg 199034, Russia
[2] Department of Mineralogy, Natural History Museum, Cromwell Road, London SW7 5BD, UK
[3] Department of Geological Sciences, University of Manitoba, Winnipeg, Manitoba R3T 2N2, Canada
[4] Department of Crystallography, Faculty of Geology, St Petersburg State University, Universitetskaya nab. 7/9, St. Petersburg 199034, Russia
[5] Department of Mineral Deposits, Faculty of Geology, St Petersburg State University, Universitetskaya nab. 7/9, St. Petersburg 199034, Russia

[*Received 6 April 2011; Accepted 23 August 2011*]

ABSTRACT

Cerianite-(Ce), ideally CeO_2, occurs as rounded grains up to 5 μm across in a block of highly altered calcite carbonatite lava from the Kerimasi volcano, and as euhedral crystals up to 200 μm across in carbonatite-derived eluvial deposits in the Kisete and Loluni explosion craters in the Gregory Rift, northern Tanzania. X-ray powder diffraction data (a = 5.434(5) Å) and Raman spectroscopy (minor vibration modes at 184 and 571 cm^{-1} in addition to a strong signal at 449 cm^{-1}) suggest the presence of essential amounts of large cations and oxygen vacancies in the Kisete material. Microprobe analyses reveal that the mineral contains both light and heavy trivalent rare earth elements (*REE*) (7.9–15.5 wt.% $LREE_2O_3$ and 4.9–9.7 wt.% $HREE_2O_3$), and that it is enriched in yttrium (7.1–14.5 wt.% Y_2O_3) and fluorine (2.2–3.5 wt.%). Single-crystal structure refinement of the mineral confirms a fluorite-type structure with a cation–anion distance of 2.3471(6) Å. The cerianite-(Ce) is considered to be a late-stage secondary mineral in the carbonatitic rocks.

Keywords: cerianite-(Ce), ceria, oxyfluoride, carbonatite, Raman spectroscopy, chemical composition, X-ray diffraction, crystal structure, Kerimasi, Kisete, Loluni, Tanzania.

Introduction

Cerianite-(Ce), ideally CeO_2, was originally described from a xenolith in a carbonatite dyke cross-cutting "nephelinised hybrid gneiss" at Lackner Lake, Ontario, Canada (Graham, 1955). It has been identified as a secondary mineral at many localities worldwide, including weathered phonolites and nepheline syenites at Morro do Ferro, Brazil (Frondel and Marvin, 1959), hydrothermal veins of probable carbonatitic origin at Karonge, Burundi (Van Wambeke, 1977), granite pegmatite at Nesöya, East Antarctica (Matsumoto and Sakamoto, 1982), alluvial deposits on the Afu Hills pegmatites, Nigeria (Styles and Young, 1983), weathered carbonatites at Mount Weld, Australia (Lottermoser, 1987), weathered syenite at Akongo, Cameroon (Braun *et al.*, 1990), palaeosols at Flin Flon, Canada (Pan and Stauffer, 2000), skarns at Bastnäs, Sweden (Holtstam and

* E-mail: burbankite@gmail.com
DOI: 10.1180/minmag.2011.075.6.2813

© *2011 The Mineralogical Society*

Andersson, 2007), alkaline pegmatites at Mount Malosa, Malawi (Guastoni *et al.*, 2009) and metasomatic rocks of the Terskii greenstone belt, Kola, Russia (Skublov *et al.*, 2009).

Published data for cerianite-(Ce) are limited to a few chemical analyses, including some that have low analytical totals that are not accounted for and others that are normalized to 100 wt.% (Graham, 1955; Styles and Young, 1983; Pan and Stauffer, 2000; Holtstam and Andersson, 2007; Skublov *et al.*, 2009), and incomplete X-ray diffraction data (Graham, 1955; Frondel and Marvin 1959; Van Wambeke, 1977; Matsumoto and Sakamoto, 1982; Styles and Young, 1983; Holtstam and Andersson, 2007). In contrast to the natural mineral, the crystal structure and spectroscopy of synthetic CeO_2 (ceria) and its Y-, La- or Zr-doped derivatives have been studied extensively due to their application in oxide fuel cells (e.g. Anderson and Wuensch, 1973; Wang *et al.*, 1981; McBride *et al.*, 1994; Otake *et al.*, 2003; Luo *et al.*, 2006; Mazali *et al.*, 2007).

In this work, we describe a new occurrence of cerianite-(Ce) in carbonatitic rocks in northern Tanzania, and report the physical properties and the crystal-chemical characteristics of this mineral determined by a wide variety of methods, including single-crystal X-ray diffraction and Raman spectroscopy.

Occurrence and physical properties

Cerianite-(Ce) occurs in carbonatite at the Kerimasi volcano (2º52′S, 35º57′E) and carbonatite-derived eluvial deposits at the nearby Kisete (2º49′S, 36º00′E) and Loluni (2º49′S, 35º58′E) explosion craters. These volcanic structures belong to the Quaternary Lake Natron–Engaruka volcanic field in the Gregory Rift, northern Tanzania (Hay, 1983; Dawson, 2008; Zaitsev, 2010; Zaitsev *et al.*, 2010; Mattsson and Tripoli, 2011).

At the Kerimasi volcano, cerianite-(Ce) was found in one sample of calcite carbonatite lava, which occurs as a block in nephelinite agglomerate (sample K 94-27). The carbonatite consists of polycrystalline calcite (as phenocrysts, microphenocrysts and in the groundmass) with rare microphenocrysts of apatite and magnetite-magnesioferrite; fine-grained apatite is also present in the carbonatite groundmass. Cerianite-(Ce) occurs as round to oval grains up to 5 μm across, which are exclusively associated with porous groundmass apatite and an anhedral Ba-Fe-Mn hydroxide (Fig. 1*a*). The microtextural observations (mineral recrystallization and partial dissolution) and aspects of the mineralogy (i.e. the occurrence of Ba-Fe-Mn, Mn and Fe hydroxides) indicate significant alteration of the studied sample. The stable isotope composition of the calcite ($\delta^{13}C$ = −3.21‰ PDB and $\delta\ ^{18}O$ = +23.41‰ SMOW), and particularly its high $\delta^{18}O$ value, suggests intensive low-temperature isotope exchange between the rock and the groundwater.

In the eluvial deposits at Kisete and Loluni (in non-magnetic and paramagnetic fraction samples KZ 2 and LL 4), cerianite-(Ce) was found as discrete euhedral crystals and intergrowths of two

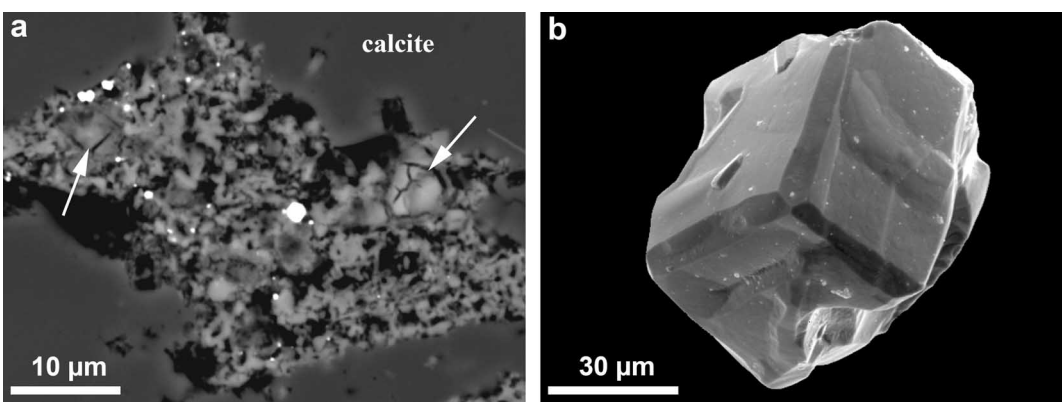

FIG. 1. Cerianite-(Ce) morphology. (*a*) Back-scattered electron image of calcite carbonatite lava from the Kerimasi volcano, sample K 94-27 showing rounded cerianite-(Ce) crystals (white) in altered groundmass apatite (grey), the arrows show Ba-Fe-Mn hydroxide. (*b*) Scanning electron microscope image showing cubic cerianite-(Ce) with dodecahedron {110} faces, from the carbonatite elluvial deposit at Kisete crater, sample KZ 2.

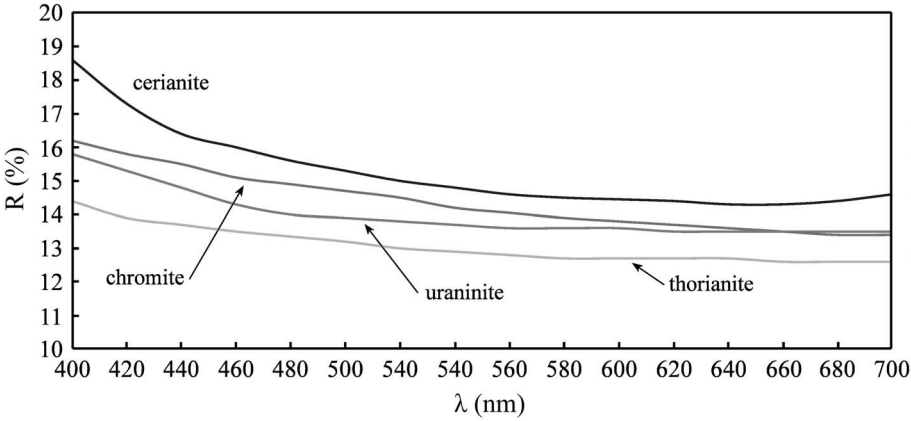

FIG. 2. Reflectance spectra for cerianite-(Ce) (sample KZ 2) with uraninite, thorianite and chromite for comparison.

or three crystals up to 200 μm in size (Fig. 1*b*). The cerianite-(Ce) is associated with diopside, schorlomite, andradite, magnetite, magnesioferrite, perovskite, apatite, pyrochlore, calzirtite, baddeleyite and kerimasite (Zaitsev *et al.*, 2010).

Cerianite-(Ce) crystals from Kisete and Loluni are cubic {100} in habit, rarely with additional dodecahedron {110} faces (Fig. 1*b*); they are light red to dark red and transparent with a vitreous lustre. The microindentation microhardness of the Kisete material (VHN_{50}) ranges from 1283 to 1397 kg/mm^2 (three measurements made on a polished single-crystal mount). The calculated density, based on the average formula and unit-cell parameters, is 6.73 g/cm^3.

In reflected light, cerianite-(Ce) is grey and isotropic with red internal reflections. Reflectance measurements were made using a SiC standard in air in the range 400–700 nm on a Zeiss Axiotron microscope. A Crystal Structures (Lanham) superstage was used to level the specimen and the standard before measurement with a J & M Tidas diode-array spectrometer. The *Onyx* software (Cavendish Instruments) produced output at intervals of 0.823 nm. The spectrum of the Kisete cerianite-(Ce) (Fig. 2; Table 1) is fairly flat and slightly higher in its reflectance levels than those of isostructural uraninite (QDF3 597) and thorianite (QDF3 574), and almost identical to that of near-endmember chromite (QDF3 95).

X-ray diffraction

Cerianite-(Ce) from the Kisete crater was initially identified by X-ray diffraction (Table 1). The data were collected at St Petersburg State University by the Gandolfi method (φ–ω rotation) using a Stoe IPDS II diffractometer equipped with an image-plate detector, Mo-Kα source and graphite monochromator, operating at 50 kV, 40 mA, with a detector-to-crystal distance of 200 mm and an exposure time of 60 min.

The unit-cell parameter of this sample (a = 5.434(5) Å), is between those for cerianite-(Ce)

TABLE 1. Reflectance percentages, powder XRD data and unit-cell parameters for cerianite-(Ce) from the Kisete crater (sample KZ 2).

λ nm	R	I_{obs}	d_{obs}	hkl
400	18.6	100	3.139	111
420	17.3	63	2.722	200
440	16.4	44	1.922	220
460	16.0	34	1.636	311
470	15.8	23	1.569	222
480	15.6	18	1.357	400
500	15.3	17	1.245	331
520	15.0	15	1.213	420
540	14.8	13	1.107	422
546	14.75	10	1.044	511
560	14.6	7	0.959	440
580	14.5	a = 5.434(5) Å		
589	14.5	V = 160.5(4) Å^3		
600	14.45			
620	14.4			
640	14.3			
650	14.3			
660	14.3			
680	14.4			
700	14.6			

from Lackner, Morro do Ferro, Karonge and Bastnäs (a = 5.41–5.42 Å; Graham, 1955; Frondel and Martin, 1959; Van Wambeke, 1977; Holtstam and Andersson, 2007), and those from the Afu Hills and Nesöya (a = 5.45–5.46 Å; Matsumoto and Sakamoto, 1982; Styles and Young, 1983). The larger unit-cell parameter of the Kisete sample in comparison with pure CeO_2 (a = 5.411–5.412 Å) can be explained by the substitution of larger trivalent lanthanide cations for Ce^{4+} (McBride *et al.*, 1994).

Raman spectroscopy

Raman spectra were collected at the University of Manitoba using an automated LabRam Aramis spectrometer operating in confocal mode, equipped with a motorized *x-y-z* stage for accurate beam positioning. Trials were made using three excitation sources with wavelengths of 532, 633 and 785 nm; the best results were obtained using the green 532 nm laser, and this was used to optimize other instrumental parameters including the slit width and spectrum acquisition time. The laser beam was aligned optically prior to the data collection, and the spectrometer calibrated using the 520 cm^{-1} peak of elemental silicon. A number of spectra were collected from the core and rim of cerianite-(Ce) crystals from the Kisete crater; one spectrum, which is shown in Fig. 3, was chosen as representative. All of the spectra exhibit identical vibration modes, but they differ slightly in their relative peak intensities.

The strong Raman signal at 449 cm^{-1} (Fig. 3), which is also observed in synthetic CeO_2 at 465 cm^{-1}, can be attributed to a symmetric breathing mode of the oxygen atoms coordinating the cerium cation (McBride *et al.*, 1994). This peak is shifted to lower frequencies in synthetic CeO_2 samples that are doped with trivalent lanthanides (McBride *et al.*, 1994). Two additional Raman peaks appear in the spectra at 184 and 571 cm^{-1} (Fig. 3); similar modes in synthetic samples of CeO_2 doped with REE^{3+} have been interpreted as an indication of the presence of oxygen vacancies (McBride *et al.*, 1994; Luo *et al.*, 2006). A weak signal at 820–825 cm^{-1} is also present in the spectra, but its origin is unclear. Importantly, the spectra of the Kisete cerianite-(Ce) lack peaks in the 3400–3600 cm^{-1} region that could be attributed to O–H stretching modes.

Composition

Quantitative microprobe analyses of five crystals of cerianite-(Ce) from Kisete were obtained using an automated CAMECA SX-100 instrument at the Natural History Museum, London (NHM). These analyses were done with a focused beam; they did not include F and gave low analytical totals. This prompted a re-investigation of the same samples using a CAMECA SX-100 at the University of Manitoba (UM). Both instruments were operated in wavelength-dispersive mode (WDS) under the following conditions: 20 kV accelerating voltage, 20 nA beam current and 1 μm beam diameter (NHM); 15 kV accelerating voltage, 20 nA beam current and 5–10 μm beam diameter (UM). The following standards were used for calibration: Ce-silicate glass and CeO_2 (Ce), *REE* silicate glasses (*REE*), jadeite (Na), wollastonite (Si, Ca) and

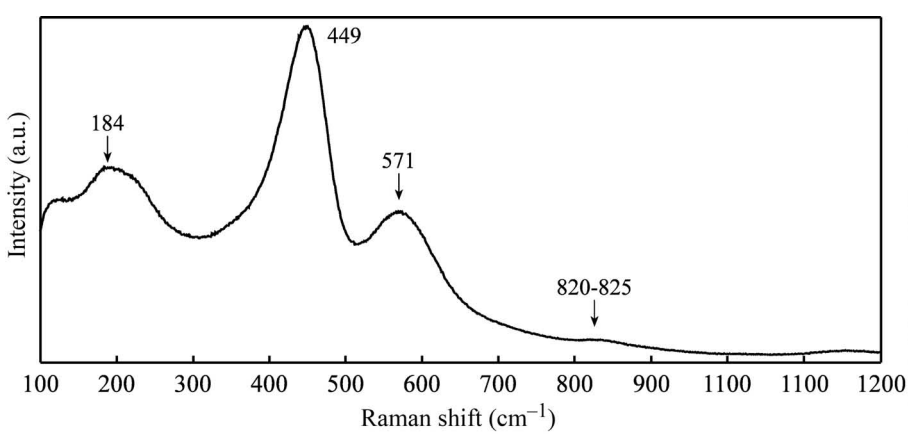

FIG. 3. The Raman spectrum of cerianite-(Ce) (sample KZ 2).

$MnTiO_3$ (Mn) at the NHM; albite (Na), diopside (Ca, Si), spessartine (Mn), topaz (F) and synthetic phosphates of individual *REE* at the UM. Corrections for element-peak overlaps were applied. Further detailed information about the instrumental conditions, including the detector types and peak positions, is available from the authors on request. At the NHM and UM, the mineral was also analysed for Al, P, K, Mg, Ti, Fe, Sr, Zr, Nb, Ta, Pb, Th and U, but none of these elements are present at detectable levels; Sc was not analysed by WDS, but careful examination of energy-dispersive spectra collected for 50 sec at 20 kV and 2 nA did not show any evidence of the Sc Kα peak at 4.1 keV.

Empirical formulae (Table 2) were calculated assuming the presence of oxygen vacancies in the Kisete cerianite-(Ce) (see 'Raman spectroscopy'). The low analytical totals ($\leqslant$97.3 wt.%) are reproducible and consistent between the two datasets obtained from same crystals at the NHM and UM, but their cause remains unclear. Raman spectra (Fig. 3) do not show any evidence of borate, carbonate or nitrate groups in the examined material and therefore, undetected B, C and N cannot be responsible for the low totals. Although the presence of Li and Be, which are not detectable by electron-microprobe analysis, cannot be ruled out, it is extremely unlikely. Damage to the sample surface produced by microprobe analysis possibly indicates that fluorine atoms were prone to beam-induced diffusion (cf. Stormer *et al.*, 1993) and that the measured F contents are, in fact, somewhat low. However, our attempts to find experimental proof of F diffusion were unsuccessful; grains in different orientations analysed using beams of different diameters yielded similar F contents.

X-ray maps of the cerianite-(Ce) crystals exhibit strongly zoned elemental distributions (Fig. 4) and microprobe analyses show that there is a significant content of trivalent rare earth elements (*REE*) (Table 2). The examined cerianite-(Ce) from Kisete is strongly enriched in Y (7.1–14.5 wt.% Y_2O_3), as well as light and heavy trivalent *REE* (7.9–15.5 and 4.9–9.7 wt.% total oxides, respectively). On the basis of Raman spectroscopy, the incorporation of trivalent elements into the Kisete material can be explained by the substitution $2Ce^{4+} + O^{2-} \leftrightarrow 2REE^{3+} + \square$. Traces of Si, Ca, Na and Mn were also found in the mineral (Table 2).

Another notable feature of the cerianite-(Ce) is the high F content, ranging between 2.2 and 3.5 wt.%, and averaging 2.7(4) wt.%. Previously, fluorine was reported in cerianite-(Ce) from Bastnäs, where its content ranges from 0.8–1.0 wt.% (Holtstam and Andersson, 2007). It is noteworthy that håleniusite, (La,Ce)OF, is isostructural with, and has a larger unit cell (a = 5.628 Å) than, synthetic CeO_2 and cerianite-(Ce) from the type locality (Graham, 1955; Holtstam *et al.*, 2004), suggesting that an appreciable amount of trivalent *REE* can be incorporated in fluorite-type oxides via the heterovalent substitution $Ce^{4+} + O^{2-} \leftrightarrow REE^{3+} + F^{-}$. In the studied Kisete material, as much as 0.31 a.p.f.u. REE^{3+} can be attributed to that substitution.

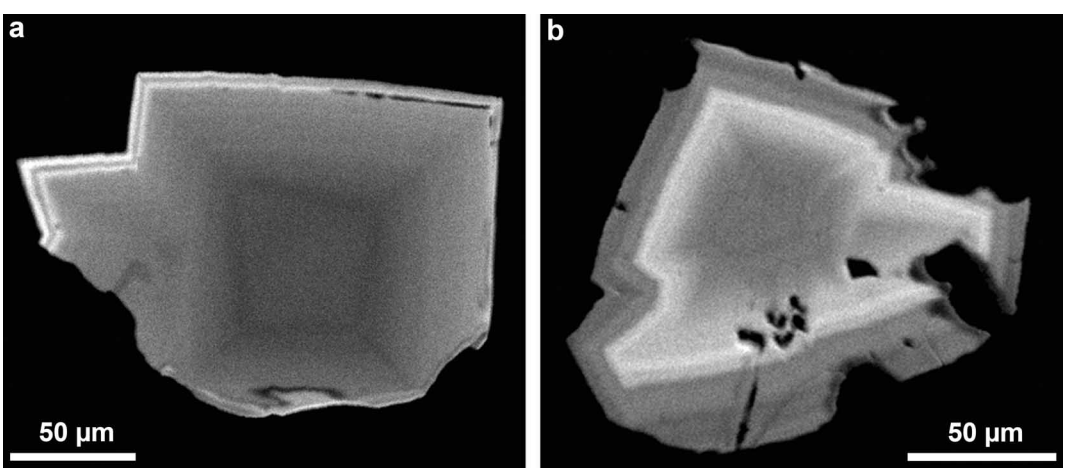

FIG. 4. Yttrium X-ray element distribution maps for zoned cerianite-(Ce) crystals (sample KZ 2).

TABLE 2. Chemical compositions of cerianite-(Ce) from the Kisete crater (sample KZ 2).

Compositions	—— 1 ——		2	—— 3 ——		4	5	6	7
Lab	UM	NHM	UM	UM	NHM	UM	UM	UM	UM
Wt.%									
La_2O_3	3.40	3.42	3.63	2.73	2.71	3.33	2.90	2.69	3.11
CeO_2	60.72	60.79	57.77	59.34	61.97	64.57	64.72	65.58	61.18
Pr_2O_3	1.31	1.79	1.60	1.49	1.68	1.36	1.28	1.40	1.23
Nd_2O_3	5.74	6.21	6.57	6.06	5.97	5.14	5.59	5.36	6.23
Sm_2O_3	1.31	1.68	1.50	1.27	1.68	1.29	1.53	1.22	1.40
Eu_2O_3	–	0.55	–	–	0.57	–	–	–	–
Gd_2O_3	1.86	1.22	1.75	2.19	1.28	1.84	1.87	1.95	2.09
Tb_2O_3	–	0.30	0.06	0.07	0.29	–	–	–	0.12
Dy_2O_3	2.22	2.06	2.15	2.01	2.13	2.18	2.09	2.19	2.56
Ho_2O_3	0.47	0.36	0.31	0.44	0.40	0.35	0.29	0.02	0.29
Er_2O_3	1.49	1.35	1.49	1.48	1.35	1.53	1.42	1.40	1.68
Tm_2O_3	0.40	0.35	0.45	0.48	0.37	0.53	0.42	0.37	0.37
Yb_2O_3	1.60	1.78	1.65	1.59	1.76	1.85	1.64	1.62	1.93
Lu_2O_3	0.65	0.34	0.65	0.38	0.31	0.64	0.50	0.80	0.67
Y_2O_3	11.65	11.93	13.68	13.41	12.24	9.46	11.16	10.72	12.19
Na_2O	0.17	0.18	0.10	0.08	0.10	0.23	0.03	0.06	0.11
SiO_2	0.55	0.64	0.17	0.06	0.25	0.63	0.05	0.12	0.19
CaO	0.24	0.23	0.14	0.11	0.12	0.28	0.10	0.12	0.16
MnO	0.18	–	0.10	0.09	–	0.18	0.13	0.09	–
F	2.96	n.a.	3.46	3.44	n.a.	2.23	2.59	2.71	2.60
$-O=F_2$	1.25		1.46	1.45		0.94	1.09	1.14	1.09
Total	95.69	95.17	95.79	95.26	95.18	96.66	97.20	97.29	97.03
Formulae calculated for cations total = 1									
La	0.035	0.035	0.038	0.029	0.028	0.034	0.030	0.028	0.032
Ce	0.594	0.587	0.568	0.589	0.605	0.627	0.636	0.644	0.596
Pr	0.013	0.018	0.016	0.015	0.017	0.014	0.013	0.014	0.013
Nd	0.057	0.061	0.066	0.062	0.060	0.051	0.056	0.054	0.062
Sm	0.013	0.016	0.015	0.012	0.016	0.012	0.015	0.012	0.014
Eu		0.005			0.005				
Gd	0.017	0.011	0.016	0.021	0.012	0.017	0.017	0.018	0.019
Tb		0.003	0.001	0.001	0.003				0.001
Dy	0.020	0.018	0.020	0.018	0.019	0.020	0.019	0.020	0.023
Ho	0.004	0.003	0.003	0.004	0.004	0.003	0.003	0.000	0.003
Er	0.013	0.012	0.013	0.013	0.012	0.013	0.013	0.012	0.015
Tm	0.004	0.003	0.004	0.004	0.003	0.005	0.004	0.003	0.003
Yb	0.014	0.015	0.014	0.014	0.015	0.016	0.014	0.014	0.016
Lu	0.006	0.003	0.006	0.003	0.003	0.005	0.004	0.007	0.006
Y	0.174	0.176	0.205	0.203	0.182	0.140	0.167	0.161	0.181
Na	0.009	0.010	0.005	0.004	0.005	0.013	0.001	0.003	0.006
Si	0.015	0.018	0.005	0.002	0.007	0.017	0.001	0.003	0.005
Ca	0.007	0.007	0.004	0.003	0.004	0.008	0.003	0.004	0.005
Mn	0.004		0.002	0.002		0.004	0.003	0.002	
Total	1.000	1.000	1.000	1.000	1.000	1.000	1.000	1.000	1.000
F	0.263	0.259	0.308	0.310	0.305	0.196	0.231	0.241	0.230
O	1.658	1.660	1.624	1.634	1.647	1.705	1.699	1.697	1.678
Total	1.921	1.919	1.932	1.943	1.951	1.902	1.930	1.938	1.907

Analyses 1–3 (Fig. 3*a*), analyses 4–6 (Fig. 3*b*).
Abbreviations are: UM, University of Manitoba laboratory; NHM, Natural History Museum laboratory; – below detection limit; n.a. – not analysed.

Single-crystal X-ray diffraction analysis

The crystal of cerianite-(Ce) from Kisete selected for single-crystal data collection was mounted on a Stoe IPDS II X-ray diffractometer operating at 50 kV and 40 mA at St Petersburg State University. More than a hemisphere of three-dimensional data was collected using monochromatic Mo-$K\alpha$ radiation, with frame widths of 2º in ω and a counting time of 120 s per frame. The unit-cell parameters of the cerianite-(Ce) (Table 3) are in general agreement with, but slightly larger than, those reported for synthetic CeO_2 by Goldschmidt and Thomassen (1923), Harwood (1949), Zintl and Croatto (1939), Brauer and Gradinger (1954) and Whitfield *et al.* (1970). To our knowledge, the present work is the first single-crystal X-ray study of natural cerianite-(Ce). The unit-cell parameters were refined using least-squares techniques. The intensity data were integrated and corrected for Lorentz polarization and background effects using *Stoe X-area* software. The observed systematic absences indicate the space group $Fm\bar{3}m$, which is in agreement with previously published data. The crystal structure of the Kisete cerianite-(Ce) was successfully refined on the basis of F^2 for all unique data using the atomic coordinates provided in the previous studies as a model. The *SHELX* software package was used for all structural calculations (Sheldrick, 2008). The final model includes all atomic positional parameters, anisotropic displacement parameters (Table 3) and a refinable weighting scheme of the structure factors. The

TABLE 3. Crystallographic data for cerianite-(Ce) from the Kisete crater.

Crystal data	
Temperature	293 K
Radiation, wavelength	Mo-$K\alpha$, 0.71073 Å
Crystal system	cubic
Space group	$Fm\bar{3}m$
Unit-cell dimension a (Å)	5.4203(14)
Unit-cell volume (Å^3)	159.25(7) Å^3
Z	4
Calculated density (g/cm^3)	6.73
Absorption coefficient	29.657 mm^{-1}
Crystal size (mm)	$0.06 \times 0.07 \times 0.07$
Data collection	
θ range	6.52−31.63º
h, k, l ranges	0−4, 0−5, 1−8
Total reflections collected	41
Unique reflections (R_{int})	32 (0.0569)
Unique reflections $F > 4\sigma(F)$	26
Structure refinement	
Refinement method	Full-matrix least-squares on F^2
Weighting coefficients a, b*	0.013400, 0.263900
Extinction coefficient	0.044(5)
Data/restraints/parameters	26/0/5
R_1 [$F > 4\sigma(F)$], wR_2 [$F > 4\sigma(F)$],	0.0071, 0.0166
R_1 all, wR_2 all	0.0071, 0.0166
Goodness-of-fit on F^2	0.987
Largest diff. peak and hole	0.36, −0.34 e Å^{-3}

Atomic coordinates and displacement parameters (Å) of atoms

Site	Site occupancy	x	y	z	U_{eq}
A	$Ce(1)^*_{0.80(6)}$ $Y(1)_{0.20(6)}$	0	0	½	0.0093(3)
X	$O(1)_{0.84}F(1)_{0.12}$	¼	¼	¼	0.0128(13)

Note: $Ce^* = Ce^{4+} + Ln^{3+}$.

final refinement converged to an agreement index (R_1) of 0.0071, calculated for the 26 unique reflections with $F > 4\sigma$ (F).

During the refinement, the occupancy of the anion X site was constrained to agree with the average compositional data. Importantly, there is no evidence for O–F ordering in the X site (see below). The refined cation occupancy of the A site by Ce* (where Ce* = Ce^{4+} + Ln^{3+}) and Y atoms (Table 3) closely matches the data obtained by WDS. The A-site cation forms eight A–X bonds with a length of 2.3471(6) Å. The fluorine content does not appear to influence the measured bond length significantly, as it is closer to that in synthetic CeO_2 (A–X = 2.343(1) Å; McCullough, 1950) than in håleniusite (A–X = 2.437(1) Å; Holstam *et al.*, 2004) or synthetic CeOF (A–X = 2.469(1) Å; Baenziger *et al.*, 1954).

The crystallography of synthetic REE^{3+} oxyfluorides (e.g. LaOF) has been studied extensively; these phases have been shown to form a variety of structure types derived from the fluorite archetype via anion ordering and polyhedral distortion. The stability of individual structure types is controlled by the synthesis temperature, the radius of the *REE* cation and non-stoichiometry at the anion site(s) (Zachariasen, 1951; Taoudi *et al.*, 1994; Juneja *et al.*, 1995; Fergus, 1997; Hölsä *et al.*, 1997). In contrast with our cerianite-(Ce), ordered synthetic oxyfluorides undergo a phase transition to a disordered cubic phase only above 530ºC (Juneja *et al.*, 1995; Anchary *et al.*, 1998; Levin *et al.*, 2005). Importantly, synthetic disordered oxyfluorides cannot be quenched to room temperature (Zachariasen, 1951; Levin *et al.*, 2005), which implies that there is a limit to the proportion of REE^{3+} and F that can be incorporated in cerianite-(Ce) and related oxides without reducing the cubic symmetry, and that the disordered structure can be effectively stabilized by smaller tetravalent cations such as Ce^{4+}.

Conclusions

Cerianite-(Ce) from carbonatite lava of Kerimasi volcano and carbonatite-derived eluvial deposits of the Kisete and Loluni explosion craters has an unusual composition relative to that reported for other localities (Graham, 1955; Styles and Young, 1983; Pan and Stauffer, 2000; Holtstam and Andersson, 2007; Skublov *et al.*, 2009). It is enriched in F (2.2–3.5 wt.%) and contains a considerable amount of Y (7.1–14.5 wt.% Y_2O_3) and trivalent lanthanides ($LREE_2O_3$ = 7.9–15.5 wt.%, $HREE_2O_3$ = 4.9–9.7 wt.%) but no detectable thorium or uranium (<1000 ppm). A significant amount of Y and *REE* in the cerianite-(Ce) and the presence of oxygen vacancies due to the substitution $2Ce^{4+} + O^{2-} \leftrightarrow 2REE^{3+} + \square$ in the mineral explain the large cell parameter and the appearance of additional vibration modes in its Raman spectrum in comparison with synthetic CeO_2. Despite the unusual cerianite-(Ce) chemistry the mineral preserves a fluorite-type structure with a cation–anion distance of 2.3471 Å.

Petrographic and mineralogical observations clearly indicate that cerianite-(Ce) from the Kerimasi volcano is a late-stage, secondary mineral that is formed as a result of the alteration of apatite. It probably precipitated from groundwater during the weathering of the carbonatite. Apatite is considered to be a major source of *REE* required for the formation of cerianite-(Ce). Electron microprobe analyses of phenocrysts and groundmass apatite from the Kerimasi and Kisete carbonatites show that it contains 0.5–1.1 wt.% $LREE_2O_3$. The crystallization of cerianite-(Ce) in the carbonatite was accompanied by Ba-Fe-Mn hydroxides (Fig. 1*a*).

Published thermodynamic calculations show that in normal geological situations, cerianite-(Ce) is stable at neutral to alkaline pH and in oxidizing conditions, i.e. positive Eh values (Braun *et al.*, 1990; Akagi and Masuda, 1998; Pan and Stauffer, 2000). The abundance of the zeolite mineral merlinoite in tuffs at the nearby Deeti explosive cone can be taken as an indication of high alkalinity of the groundwater in the area around the Kerimasi volcano and the Kisete and Loluni explosion craters (Donahoe *et al.*, 1984, 1990).

Acknowledgements

We thank A.V. Antonov and A. Kearsley for assistance with SEM observations and A. Wighton for help with sample preparation. Comments of T. Riley, F. Nestola and R.H. Mitchell improved the manuscript. This work was supported by the Alexander von Humboldt Stiftung (Germany), Natural Sciences and Engineering Research Council of Canada, Ministry of Education and Science of the Russian Federation (contract 2009-1.1-152-067-003) and St Petersburg State University (Russia).

References

Akagi, T. and Masuda, A. (1998) A simple thermodynamic interpretation of Ce anomaly. *Geochemical Journal*, **32**, 301–314.

Anderson, H.T. and Wuensch, B.J. (1973) CeO_2–Y_2O_3 solid solutions. *Journal of the American Ceramic Society*, **56**, 285–286.

Anchary, S.N., Ambekar, B.R., Mathews, M.D., Tyagi, A.K. and Moorthy, P.N. (1998) Study of phase transition and volume thermal expansion in a rare-earth (RE) oxyfluoride system by high-temperature XRD (RE=La, Nd, Sm, Eu and Gd). *Thermochimica Acta*, **320**, 239–243.

Baenziger, N.C., Holden, J.R., Knudson, G.E. and Popov, A.I. (1954) Unit cell dimensions of some rare earth oxyfluorides. *Journal of the American Chemical Society*, **76**, 4734–4735.

Brauer, G. and Gradinger, H. (1954) Über heterotype Mischphasen bei Seltenerdoxyden. II. Die Oxydsysteme des Cers und des Praseodyms. *Zeitschrift für Anorganische und Allgemeine Chemie*, **277**, 89–95.

Braun, J.-J., Pagel, M., Muller, J.-P., Bilong, P., Michard, A. and Guillet, B. (1990) Cerium anomalies in lateritic profiles. *Geochimica et Cosmochimica Acta*, **54**, 781–795.

Dawson, J.B. (2008) *The Gregory rift valley and Neogene-recent volcanoes of northern Tanzania*. Memoir of the Geological Society of London, **33**. The Geological Society, London, 102 pp.

Donahoe, R.J., Liou, J.G. and Guldman, S. (1984) Synthesis and characterization of zeolites in the system Na_2O–K_2O–$A1_2O_3$–SiO_2–H_2O. *Clays and Clay Minerals*, **32**, 433–443.

Donahoe, R.J., Liou, J.G., and Hemingway, B.S. (1990) Thermochemical data for merlinoite: 2. Free energies of formation at 298.15 K of six synthetic samples having various Si/Al and Na/(Na + K) ratios and application to saline, alkaline lakes. *American Mineralogist*, **75**, 201–208.

Fergus, J.W. (1997) Crystal structure of lanthanum oxyfluoride. *Journal of Materials Science Letters*, **16**, 267–269.

Frondel, C. and Marvin, U.B. (1959) Cerianite, CeO_2, from Peços de Caldas, Brazil. *American Mineralogist*, **44**, 882–884.

Goldschmidt, V.M. and Thomassen, L. (1923) *Die Krystallstruktur natürlicher und synthetischer Oxyde von Uran, Thorium und Cerium*. Videnskapsseiskapets Skrifter. I. Matematisk-Naturvidenskapelig Klasse, No. 2. Kristiania: Jacob Dybwad, Oslo, 48 pp.

Graham, A.R. (1955) Cerianite CeO_2: a new rare-earth oxide mineral. *American Mineralogist*, **40**, 560–564.

Guastoni, A., Nestola, F. and Giaretta, A. (2009) Mineral chemistry and alteration of rare earth element (REE) carbonates from alkaline pegmatites of Mount Malosa, Malawi. *American Mineralogist*, **94**, 1216–1222.

Harwood, M.G. (1949) Variation in density and colour of cerium oxide. *Nature*, **164**, 787.

Hay, R.L. (1983) Natrocarbonatite tephra of Kerimasi volcano, Tanzania. *Geology*, **11**, 599–602.

Hölsä, J., Säilynoja, E., Rahiala, H. and Valkonen, J. (1997) Characterization of the non-stoichiometry in lanthanum oxyfluoride by FT-IR absorption, Raman scattering, X-ray powder diffraction and thermal analysis. *Polyhedron*, **16**, 3421–3427.

Holtstam, D. and Andersson, U.B. (2007) The REE minerals of the Bastnäs-type deposits, south-central Sweden. *The Canadian Mineralogist*, **45**, 1073–1114.

Holtstam, D., Grins, J. and Nysten, P. (2004) Håleniusite-(La) from the Bastnäs deposit, Västmanland, Sweden: a new REE oxyfluoride mineral species. *The Canadian Mineralogist*, **42**, 1097–1103.

Juneja, J.M., Tyagi, A.K., Chattopadhyay, G. and Seetharaman, S. (1995) Sub-solidus phase equilibria in the NdF_3-Nd_2O_3 system. *Materials Research Bulletin*, **30**, 1153–1160.

Levin, I., Huang, Q.Z., Cook, L.P. and Wong-Ng, W. (2005) Nonquenchable chemical order-disorder phase transition in yttrium oxyfluoride. *European Journal of Inorganic Chemistry*, **2005**, 87–91.

Lottermoser, B.G. (1987) Churchite from the Mt Weld carbonatite laterite, Western Australia. *Mineralogical Magazine*, **51**, 468–469.

Luo, M.F., Yan, Z.-L. and Jin, L.-Y. (2006) Structure and redox properties of $Ce_\chi Pr_{1-\chi}O_{2-\delta}$ mixed oxides and their catalytic activities for CO, CH_3OH and CH_4 combustion. *Journal of Molecular Catalysis A: Chemical*, **260**, 157–162.

Matsumoto, Y. and Sakamoto, A. (1982) Preliminary report on metamict cerianite from Nesöya, Lützow-Holmbukta, East Antarctica. *Memoirs of National Institute of Polar Research*, **21**, 103–111.

Mattsson, H.B. and Tripoli, B.A. (2011) Depositional characteristics and volcanic landforms in the Lake Natron–Engaruka monogenetic field, northern Tanzania. *Journal of Volcanology and Geothermal Research*, **203**, 23–34.

Mazali, I.O., Viana, B.C., Alves, O.L., Mendes Filho, J. and Souza Filho, A.G. (2007) Structural and vibrational properties of CeO_2 nanocrystals. *Journal of Physics and Chemistry of Solids*, **68**, 622–627.

McBride, J.R., Hass, K.C., Poindexter, B.D. and Weber, W.H. (1994) Raman and x-ray studies of $Ce_{1-x}RE_xO_{2-y}$, where RE=La, Pr, Nd, Eu, Gd, and Tb. *Journal of Applied Physics*, **76**, 2435–2441.

McCullough, J. D. (1950) An X-ray study of the rare-

earth oxide systems: Ce^{IV}–Nd^{III}, Ce^{IV}–Pr^{III}, Ce^{IV}–Pr^{IV} and Pr^{IV}–Nd^{III}. *Journal of the American Chemical Society*, **72**, 1386–1386.

Otake, T., Yugami, H., Yashiro, K., Nigara, Y., Kawada, T. and Mizusaki, J. (2003) Nonstoichiometry of $Ce_{1-X}Y_XO_{2-0.5X-\delta}$ (X=0.1, 0.2). *Solid State Ionics*, **161**, 181–186.

Pan, Y. and Stauffer, M.R. (2000) Cerium anomaly and Th/U fractionation in the 1.85 Ga Flin Flon Paleosol: clues from *REE*- and U-rich accessory minerals and implications for paleoatmospheric reconstruction. *American Mineralogist*, **85**, 898–911.

Sheldrick, G.M. (2008) A short history of *SHELX*. *Acta Crystallographica*, **A64**, 112–122.

Skublov, S.G., Astaf'ev, B.Yu., Marin, Yu.B., Gembitskaya, I.M. and Levchenkov, O.A. (2009) First find of cerianite in zircons from metasomatites of the Terskii Greenstone Belt, Baltic Shield. *Doklady Earth Sciences*, **428**, 1134–1138.

Stormer, J.C. Jr., Pierson, M.L. and Tacker, R.C. (1993) Variation of F and Cl X-ray intensity due to anisotropic diffusion in apatite during electron microprobe analysis. *American Mineralogist*, **78**, 641–648.

Styles, M.T. and Young, B.R. (1983) Fluocerite and its alteration products from the Afu Hills, Nigeria. *Mineralogical Magazine*, **47**, 41–46.

Taoudi, A., Laval, J.P. and Frit, B. (1994) Synthesis and crystal structure of three new rare earth oxyfluorides related to baddeleyite (LnOF; Ln=Tm, Yb, Lu). *Materials Research Bulletin*, **29**, 1137–1147.

Van Wambeke, L. (1977) The Karonge rare earth deposits, Republic of Burundi: new mineralogical-geochemical data and origin of the mineralization. *Mineralium Deposita*, **12**, 373–380.

Wang, D.Y., Park, D.S., Griffith, J. and Nowick, A.S. (1981) Oxygen-ion conductivity and defect interactions in yttria-doped ceria. *Solid State Ionics*, **2**, 95–105.

Whitfield, H.J., Roman, D. and Palmer, A.R. (1970) X-ray study of the system ThO_2–CeO_2–Ce_2O_3. *Journal of Inorganic and Nuclear Chemistry*, **28**, 2817–2825.

Zachariasen, W.H. (1951) Crystal chemical studies of the 5*f*-series of elements. XIV. Oxyfluorides, *X*OF. *Acta Crystallographica*, **4**, 231–236.

Zaitsev, A.N. (2010) Nyerereite from calcite carbonatite at the Kerimasi volcano, northern Tanzania. *Geology of Ore Deposits*, **52**, 630–640.

Zaitsev, A.N., Williams, C.T., Britvin, S.N., Kuznetsova, I.V., Spratt, J., Petrov, S.V. and Keller, J. (2010) Kerimasite, $Ca_3Zr_2(Fe_2^{3+}Si)O_{12}$, a new garnet from carbonatites of Kerimasi volcano and surrounding explosion craters, northern Tanzania. *Mineralogical Magazine*, **74**, 803–820.

Zintl, E. and Croatto, U. (1939) Fluoritgitter mit leeren Anionenplätzen. *Zeitschrift für Anorganische und Allgemeine Chemie*, **242**, 79–86.